ISSN 0023-1584, Kinetics and Catalysis, 2007, Vol. 48, No. 5, pp. 620–625. © MAIK "Nauka/Interperiodica" (Russia), 2007.
Original Russian Text © I.K. Larin, A.I. Spasskii, E.M. Trofimova, L.E. Turkin, 2007, published in Kinetika i Kataliz, 2007, Vol. 48, No. 5, pp. 664–669.

Reactions of the $IO^{\bullet}$ Radical Resulting in Hydrogen Atom Abstraction from Halogen-Containing Molecules

I. K. Larin, A. I. Spasskii, E. M. Trofimova, and L. E. Turkin

Institute of Energy Problems of Chemical Physics, Russian Academy of Sciences, Chernogolovka, Moscow oblast, 142432 Russia

e-mail: emtrofimova@mtu-net.ru

Received September 7, 2006

Abstract—A jet-stream kinetic technique and the resonance fluorescence method applied to detection of iodine atoms were used to measure the rate constants of the reactions of the $IO^{\bullet}$ radical with the halohydrocarbons CHFCl–CF_2Cl ($k = (3.2 \pm 0.9) \times 10^{-16}$ cm^3 molecule s^{-1}) and CH_2ClF ($k = (9.4 \pm 1.3) \times 10^{-16}$ cm^3 molecule s^{-1}), the hydrogen-containing haloethers CF_3–O–CH_3 ($k = (6.4 \pm 0.9) \times 10^{-16}$ cm^3 molecule s^{-1}) and CF_3CH_2–O–CHF_2 ($k = (1.2 \pm 0.6) \times 10^{-15}$ cm^3 molecule s^{-1}), and hydrogen iodide ($k = (1.3 \pm 0.9) \times 10^{-12}$ cm^3 molecule s^{-1}) at 323 K.

DOI: 10.1134/S0023158407050035

INTRODUCTION

Reactions of the $IO^{\bullet}$ radical with hydrogen-containing organic and inorganic compounds evoke interest because, due to the Hal–O bond strength decreasing in the order $ClO^{\bullet} > BrO^{\bullet} > IO^{\bullet}$, $IO^{\bullet}$ is a stronger oxidizer than $BrO^{\bullet}$ or $ClO^{\bullet}$ and the H–O bond strength increases in the order H–OCl < H–OBr < H–OI. The energy of the bond between $IO^{\bullet}$ and the H atom in HOI is 459 kJ/mol [1] and exceeds the H bonding energy in many natural and anthropogenic hydrogen-containing atmospheric components. This fact raised the hope that $IO^{\bullet}$ could react with hydrogen-containing components at a noticeable rate. This would necessitate revising the conventional views of the sink of atmospheric RH components and the current estimates of the lifetimes of these compounds in the atmosphere. Iodine was earlier believed to play a significant role only in tropospheric chemistry because the iodine-containing compounds are short-lived and undergo photodecomposition within the troposphere [2]. However, iodine-containing compounds were later demonstrated to reach the stratosphere owing to convective flows, particularly in the tropics, and to be involved in the catalytic destruction of stratospheric ozone [3].

It was postulated [4] that the $IO^{\bullet}$ radical can react with organic molecules to abstract a hydrogen atom, yielding HOI. The formation of HOI was detected [5] in the reaction

$$IO^{\bullet} + CH_3SH \longrightarrow HOI + CH_3S^{\bullet}, \qquad (I)$$

whose rate constant was determined to be $k_1 = 6 \times 10^{-16}$ cm^3 molecule s^{-1}. The reactions of the $IO^{\bullet}$ radical with C_2H_4 and C_2H_6 were also studied [5]. No hydrogen abstraction was observed, indicating that the rate constant is lower than 2×10^{-16} cm^3 molecule s^{-1}. No addition to the double bond was observed, contrary to the case of the reactions of the $OH^{\bullet}$ radical with these substances.

Presently, the $OH^{\bullet}$ radical is considered to be the only tropospheric "cleaner" incompletely destructing halogen-substituted hydrocarbons via the reaction

$$R–H + OH^{\bullet} \longrightarrow H_2O + R^{\bullet}. \qquad (II)$$

Thus, this is precisely reaction (II) that determines the lifetime of these compounds in the atmosphere and, hence, their contribution to ozone layer degradation and the greenhouse effect. However, simulations [6] demonstrated that the global average concentration of the $IO^{\bullet}$ radical in the troposphere can be comparable with that of $OH^{\bullet}$. Therefore, for reliable description of atmospheric processes, it is necessary to elucidate whether the tropospheric sink via the reaction

$$IO^{\bullet} + RH \longrightarrow HOI + R^{\bullet} \qquad (III)$$

can compete with the sink via reaction (II); that is, it necessary to elucidate whether the reactions of hydrogen-containing haloalkanes with the $IO^{\bullet}$ radical should be taken into account in the calculation of the lifetimes of the haloalkanes and in the estimation of their contribution to ozone depletion and the greenhouse effect.

The rate constants of the reactions of the IO• radical with $CHCl_2$–CF_2Cl (k = (4.9 ± 0.9) × 10^{-16} cm^3 molecule s^{-1} at 303 K) and formic acid (k = (29.5 ± 12) × 10^{-16} cm^3 molecule s^{-1} at 323 K) were measured [7] under flow conditions using the resonance fluorescence method to detect iodine atoms.

In this work, we used the same procedure to measure the rate constants of the reactions of the IO• radical with the halohydrocarbons CHFCl–$CClF_2$ and CH_2ClF, the ethers CF_3–O–CH_3 and CF_3CH_2–O–CHF_2, and hydrogen iodide.

EXPERIMENTAL

Jet-Stream Kinetic Technique Using Resonance Fluorescence for Detection of Iodine Atoms

The resonance fluorescence method used in the detection of iodine atoms made it possible to study processes involving iodine atoms and IO• radicals at low iodine atom concentrations of ~10^7–10^8 atom/cm^3, at which any contribution from secondary reactions (particularly the very fast recombination of IO• radicals) can be ruled out.

The jet-stream kinetic technique was detailed earlier [8]. Here we present a brief description. The apparatus consists of a flow reactor (Fig. 1), a source of iodine atoms, an iodine atom detection system, and a feed system making it possible to maintain constant reactant flow rates with an accuracy of about 2–3% during the experiment (10–15 h).

The reactor (Fig. 1) is a cylindrical quartz tube 1.5 cm in diameter, whose inner surface is lined with F-32-L fluoroplastic to reduce the heterogeneous loss of IO• radicals and iodine atoms. The reactor has a water jacket for temperature control between 273 and 360 K. The reactor temperature was maintained higher than room temperature (323 K) to reduce the heterogeneous loss of IO• radicals. Gases (reactants and carriers) were introduced through side inlets in the upper part of the reactor. Iodine atoms were introduced at various distances from the detection zone through a nozzle movable along the reactor axis.

Iodine atoms were obtained by the photolysis of CH_3I at λ = 253.7 nm with a low-pressure mercury lamp. The source of iodine atoms was a quartz tube 1.5 cm in diameter, whose surface was covered with orthophosphoric acid. The mercury lamp was parallel to the tube of the source. The mobile source of iodine atoms was a single whole with the mobile nozzle and moved together with it.

The iodine atom detection system consisted of a resonance lamp, whose radiation corresponded to the resonance line of the iodine atom (178.3 nm), a detection zone containing iodine atoms, a photoionization counter for detecting photons reemitted by the iodine atoms, and a Ch3-63/1 frequency meter connected with a computer.

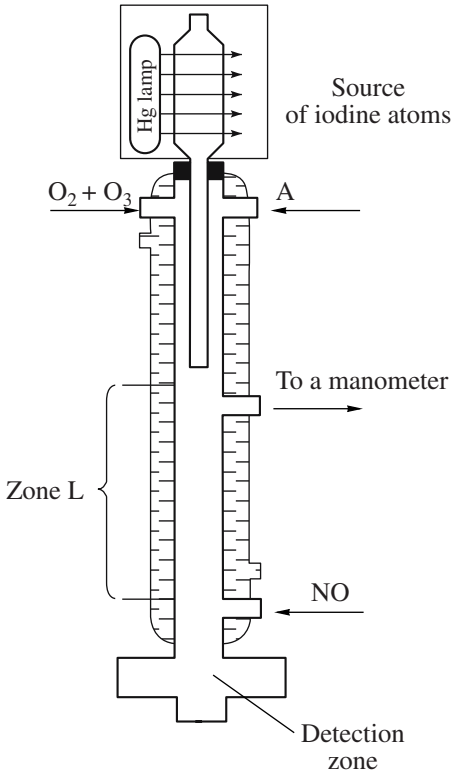

Fig. 1. Schematic of the reactor.

The flow-through iodine resonance lamp was a quartz tube, through which an I_2/He mixture (1 : 10000) was pumped with a velocity of 3500 cm/s at 1.6 Torr. A Breid microwave resonator (254 MHz, 2.5 W) was used to initiate a discharge in the lamp. The light from the resonance lamp was absorbed by iodine atoms in the detection zone. This zone consisted of tubes 10 mm in diameter and 10 mm in length soldered crosswise into the reactor. The tubes ended with quartz sockets, in which the brass cones of a resonance lamp and of a photon counter and glass Wood horns were secured. The Wood horns served to reduce the backscatter of resonance radiation.

The ionization counter was filled with a mixture of Ar, NO, and diethylferrocene. The operating frequency range was 165–185 nm. The resonance radiation absorption cross section of the iodine atom at λ = 178.3 nm is $\sigma^{res}_{\lambda = 178.3} = 5 \times 10^{-13}$ cm^2 [9], and the reemitted quantum value (6.9 eV) is rather high. This allowed photoionization counters requiring no monochromator to be used as a reemitted light detector.

To obtain ozone, a He + 4% O_2 mixture was passed through an Ozon-2 ozonizer. The ozone-enriched mixture was passed through a 10-cm-long glass cell with quartz windows placed in a Spectromom-204 spectrophotometer. Absorbance at λ = 253.7 nm was moni-

tored. The amount of ozone entering the reactor in 1 s was determined using the formula

$$Q(O_3) = Q(O_2 + He)\frac{2.3D_{10}}{3.25 \times 10^{16}\sigma L_{cell}P_{cell}} \quad (1)$$

$$[cm^3\ Torr\ s^{-1}],$$

where $Q(O_2 + He)$ is the total flow rate in the ozonizer line (cm^3 Torr s^{-1}), D_{10} is absorbance in decimal logarithms (spectrophotometer reading), $\sigma_{253.7} = 1.15 \times 10^{-17}$ cm^2 is the absorption cross section of ozone at $\lambda = 253.7$ nm, L_{cell} is the optical path length of the cell, and P_{cell} is the gas pressure in the cell (Torr).

The absolute sensitivity of this technique to iodine atoms was calibrated before each series of experiments. The absolute sensitivity of the technique in different series of experiments varied between 3×10^7 and 10^8 cm^{-3} at a signal-to-noise ratio of 1 and a pulse accumulation time of ~100 s.

Study of Reactions of the IO• Radical with Hydrogen-Containing Compounds without Formation of Iodine Atoms (Procedure 1)

The reaction rate constant was determined as follows: iodine atoms (~1×10^{10} atom/cm^3) were introduced through the mobile nozzle into a dioxygen flow containing ~1×10^{15} molecule/cm^3 of ozone. Iodine atoms could be introduced into the flow at different distances from the detection zone. The IO• radical resulted from the fast reaction

$$I + O_3 \xrightarrow{k_4} IO^\bullet + O_2, \quad (IV)$$

whose rate constant at the experimental temperature was $k_4 = 1.2 \times 10^{-12}$ cm^3/s [10]. Due to this reaction and iodine loss on the walls,

$$I + wall \xrightarrow{k_5} products, \quad (V)$$

the concentration of iodine atoms decreased rapidly according to the expression

$$\ln([I]/[I]_0) = -(k_4[O_3] + k_5)t. \quad (2)$$

The characteristic time of 98% conversion was

$$\tau_{98} = -\frac{\ln 0.02}{k_4[O_3] + k_5} < \frac{4}{k_4[O_3]}. \quad (3)$$

Expression (2) is independent of the IO• loss on the walls if there are no reactions converting IO• back into iodine. Thus, it can be seen from Eq. (3) that 98% of the iodine atoms were surely converted into IO• in a time equal to the quadruple characteristic time of reaction (IV).

The typical conversion length in our experiments was ~0.25 cm. Thus, at a distance of 1 cm from the nozzle cut, 98% of the iodine atoms were converted into IO• radicals. The zone L, whose upper boundary was at a distance of 1 cm from the nozzle cut and whose lower boundary coincided with the inlet through which NO was fed into the reactor, is shown in Fig. 1. In the zone L, all of the active iodine exists as IO• . The length of the zone L could be varied between 0 and 20 cm by moving the nozzle. The concentration of the IO• radicals at the entrance end of the zone L ($[IO^\bullet]_0$) was equal to the concentration of iodine atoms introduced through the nozzle. The change in the IO• concentration across the zone L was determined by the heterogeneous loss reaction

$$IO + wall \xrightarrow{k_6} products \quad (VI)$$

and by the reaction between the IO• radical and the RH molecule (reaction (III)).

Let the concentration of IO• radicals at the exit end of the zone L be designated $[IO^\bullet]_{fin}$. At the exit end of the zone L, NO (~10^{14} cm^{-3}) was fed into the vessel through a side inlet. The IO• radicals that had not reacted in the zone L entered into a chain reaction, whose first step was

$$IO + NO \xrightarrow{k_7} I + NO_2 \quad (VII)$$

and whose second step was reaction (IV).

The characteristic time of the establishment of the steady-state concentrations of iodine atoms and IO• radicals ($[IO^\bullet]_{st}$, $[I]_{st}$), which obeyed the equation

$$k_7[IO]_{st}[NO] = k_4[I]_{st}[O_3], \quad (4)$$

was $\tau \sim 1/(k_7[NO] + k_4[O_3]) \sim 3 \times 10^{-4}$ s. Since the IO• concentration at the exit end of the zone L, $[IO^\bullet]_{fin}$, is

$$[IO^\bullet]_{fin} = [IO^\bullet]_{st} + [I]_{st}, \quad (5)$$

it can readily be seen that the steady-state concentration of iodine atoms in the detection zone is related to $[IO^\bullet]_{fin}$ by the equation

$$[I]_{st} = [IO]_{fin}\frac{k_7[NO]}{k_4[O_3] + k_7[NO]} = \alpha[IO]_{fin}. \quad (6)$$

Thus, the iodine atom concentration detected by the resonance fluorescence method, $[I]_{st}$, was proportional to the IO• concentration at the exit end of the zone L.

The proportionality coefficient was determined only by the NO and O_3 concentrations, which were constant in each entry, and was independent of the nozzle position or the RH concentration added to the flow. From entry to entry, α varied between 0.67 and 0.88. After NO was introduced into the flow, the following reaction could occur along with reactions (VII) and (IV):

$$I + NO + O_2 \xrightarrow{k_8} INO + O_2. \quad (VIII)$$

This reaction would decrease the concentration of iodine atoms in the detection zone. Its rate constant is $k_8 = 2.7 \times 10^{-32}$ cm^3/s [11], and its characteristic time is longer than 1 s under the experimental conditions examined, whereas the time of flight of the reaction mixture from the NO inlet to the detection zone is ~10^{-2} s. Therefore, the consumption of atomic iodine in reaction (VIII) did not exceed 0.5%.

Neglecting the axial diffusion and radial distribution of active species, we can represent the variation of the IO• concentration along the reactor axis as

$$\ln[\mathrm{IO}^\bullet]_{\mathrm{fin}} = \ln[\mathrm{IO}^\bullet]_0 - (k_6 + k_3[\mathrm{RH}])\tau, \qquad (7)$$

where $[\mathrm{IO}^\bullet]_0$ and $[\mathrm{IO}^\bullet]_{\mathrm{fin}}$ are the initial and final concentrations of IO• radicals, [RH] is the concentration of the hydrogen-containing reactant (added in excess), $\tau = L/v$ is the residence time of the reactants, L is the distance between the iodine atom inlet nozzle and the NO introduction point, and v is the weight-average flow rate. Since, according to expression (6), the resonance fluorescence signal intensity I is proportional to $[\mathrm{IO}^\bullet]_{\mathrm{fin}}$, Eq. (7) can be rewritten as

$$\ln I = \mathrm{const} - (k_6 + k_3[\mathrm{RH}])\tau = \mathrm{const} - k_{\mathrm{eff}}\tau. \qquad (8)$$

Reactions of the IO• Resulting in Atomic Iodine Formation (Procedure 2)

Procedure 2 was detailed in an earlier publication [12]. Here we present only a brief description. Atomic iodine, whose concentration was proportional to the resonance fluorescence signal, was fed into the reactor. A chain process including two chain propagation steps, namely, reactions (IV) and (a), occurred in the reactor:

$$\mathrm{IO} + \mathrm{A} \xrightarrow{k_\mathrm{A}} \mathrm{AO} + \mathrm{I}. \qquad (a)$$

In the absence of an additional source of iodine atoms or a noticeable sink of active iodine (chain termination reactions) and when reaction (a) is homogeneous, the steady-state concentrations of iodine atoms and IO• radicals are related by the equation

$$[\mathrm{I}]_{\mathrm{st}} + [\mathrm{IO}]_{\mathrm{st}} = [\mathrm{I}]_0, \qquad (9)$$

where $[\mathrm{I}]_0$ is the initial concentration of iodine atoms.

The stationarity condition

$$k_4[\mathrm{I}][\mathrm{O_3}] = k_\mathrm{A}[\mathrm{IO}^\bullet][\mathrm{A}] \qquad (10)$$

makes it possible to obtain, using expression (4), the simple equation

$$\frac{[\mathrm{I}]_0}{[\mathrm{I}]_{\mathrm{st}}} = \frac{k_4[\mathrm{O_3}]}{k_\mathrm{A}[\mathrm{A}]} + 1. \qquad (11)$$

Note again that Eq. (6) is applicable only to homogeneous reaction (a) and only in the absence of disregarded active species loss or generation reactions.

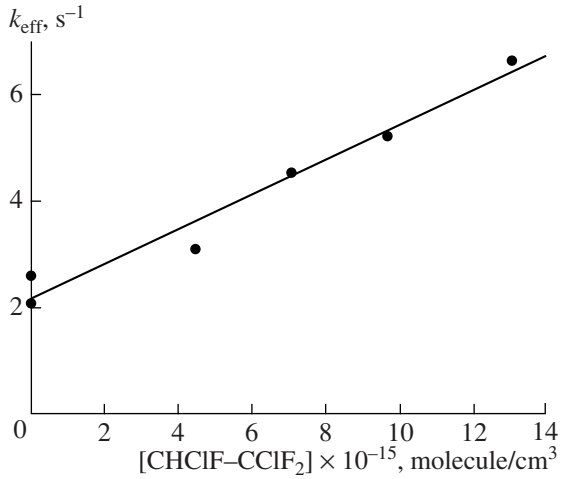

Fig. 2. Plot of k_{eff} versus the CHFCl–CF_2Cl concentration.

In our works, these conditions have been fulfilled only for the reaction of IO• with nitrogen oxide (NO), for which the plot of I_0/I_{st} versus $[O_3]/[A]$ always intersects the ordinate axis at $y = 1$ [13] ($I_0/I_{\mathrm{st}} = [\mathrm{I}]_0/[\mathrm{I}]_{\mathrm{st}}$).

For various reactions, this plot intersects the ordinate axis well above $y = 1$ because these reactions are inhomogeneous. Mathematical processing of the experimental data, which was described in detail in earlier papers [12, 14], made it possible to separate the homogeneous component and the heterogeneous component of the rate constant of reaction (a).

If there are extra sources of active species, the plot of I_0/I_{st} versus $[O_3]/[A]$ will intersect the ordinate axis at $y < 1$ because of I_{st} exceeding I_0.

RESULTS AND DISCUSSION

Reactions of IO• with Halohydrocarbons

The rate constant of the reaction

$$\mathrm{IO}^\bullet + \mathrm{CHFClCF_2Cl} \xrightarrow{k_9} \mathrm{HOI} + \mathrm{CFClCF_2Cl} \qquad (\mathrm{IX})$$

was determined at $T = 323$ K, $P = 2.85$ Torr, and $[O_3] = 5.5 \times 10^{14}$ molecule/cm^3. The plot of k_{eff} versus the CHClF–$CClF_2$ concentration is shown in Fig. 2. The rate constant of reaction (IX) at 323 K determined by the least squares method is $k_9 = (3.2 \pm 0.4) \times 10^{-16}$ cm^3 molecule s^{-1}.

Under the same conditions, we measured the rate constant of the reaction between CH_2ClF and IO• (Fig. 3): $k = (9.8 \pm 0.4) \times 10^{-16}$ cm^3 molecule s^{-1}.

Reactions of IO• with Incompletely Substituted Haloethers

The reactions of the IO• radical with incompletely substituted haloethers, another class of hydrogen-con-

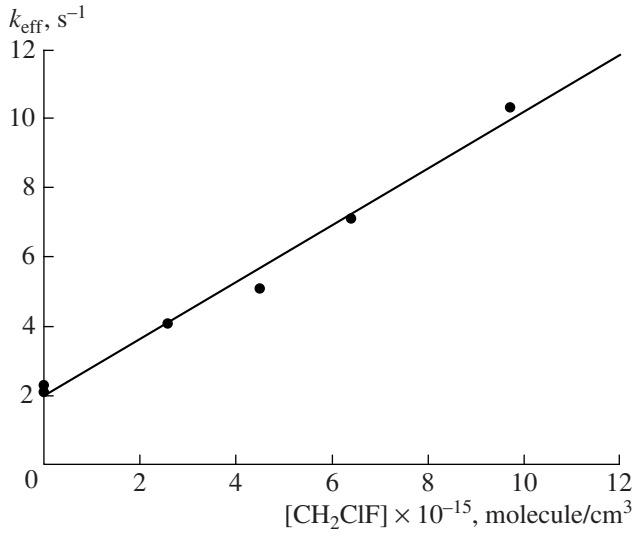

Fig. 3. Plot of k_{eff} versus the CH_2ClF concentration.

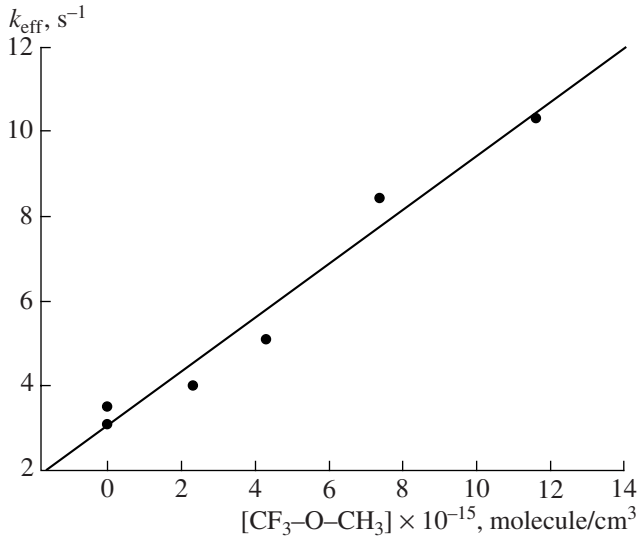

Fig. 4. Plot of k_{eff} versus the $CF_3–O–CH_3$ concentration.

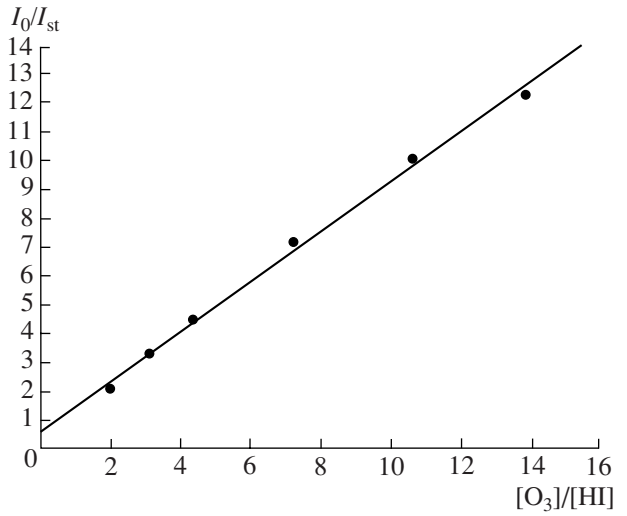

Fig. 5. Plot of I_0/I_{st} versus $[O_3]/[HI]$ for reaction (XII).

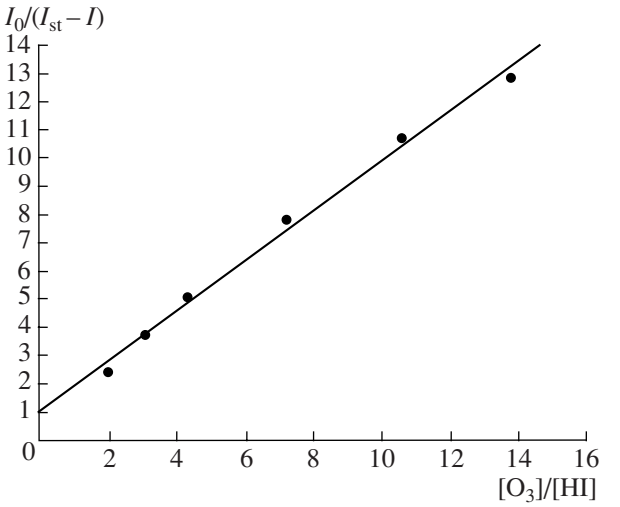

Fig. 6. Plot of $I_0/(I_{st} - I)$ versus $[O_3]/[HI]$ for reaction (XII).

taining organic compounds, were studied using procedure 1.

The reaction involving ether $CF_3–O–CH_3$ was carried out at $P = 2.8$ Torr and an ozone concentration of $[O_3] = 5.5 \times 10^{14}$ molecule/cm^3. The rate constant of the reaction

$$IO^{\cdot} + CF_3OCH_3 \xrightarrow{k_{10}} HOI + CF_3OCH_2 \qquad (X)$$

was $k_{10} = (6.4 \pm 0.9) \times 10^{-16}$ cm^3 molecule s^{-1}. The plot of k_{eff} versus the ether concentration is shown in Fig. 4.

For $CF_3CH_2–O–CHF_2$ at $[O_3] = 5.0 \times 10^{14}$ molecule/cm^3 and $P = 2.5$ Torr, the rate constant of the reaction

$$IO^{\cdot} + CF_3CH_2OCHF_2 \xrightarrow{k_{11}} HOI + CF_3CH_2OCF_2 \quad (XI)$$

was $k_{11} = (1.2 \pm 0.6) \times 10^{-16}$ cm^3 molecule s^{-1}.

Reaction between $IO^{\cdot}$ and Hydrogen Iodide

The reaction of $IO^{\cdot}$ with hydrogen iodide,

$$IO^{\cdot} + HI \xrightarrow{k_{12}} I + HOI, \qquad (XII)$$

was studied at 323 K using procedure 2.

The plot of I_0/I_{st} versus $[O_3]/[HI]$ is shown in Fig. 5. It can be seen that the straight line intersects the ordinate axis at $y < 1$. We assumed that iodine atoms can also result from the reaction between hydrogen iodide and ozone, and this assumption was confirmed by subsequent experiments. When the source of iodine atoms was switched off, we observed the resonance fluores-

cence signal of iodine atoms, which was different from the background signal and depended on the hydrogen iodide concentration. The relevant experimental data are presented below.

$[HI] \times 10^{-14}$, molecule/cm^3	2.6	1.74	1.24	0.75	0.51	0.39
I, pulse/10 s	40	22	14	7	4	3

I is the signal measured when the iodine source is switched off.

The plot of $I_0/(I_{st} - I)$ versus $[O_3]/[HI]$ is presented in Fig. 6. The rate constant of reaction (XII) was derived from the slope of the line and turned out to be $k_{12} = (1.3 \pm 0.25) \times 10^{-12}$ cm^3 molecule s^{-1}.

Thus, while the $IO^{\cdot}$ radical–hydrogen iodide reaction yielding HOI (reaction (XII)) can occur at a high rate, the reactions of $IO^{\cdot}$ with halohydrocarbons and hydrogen-containing haloethers are slow and the sink of the hydrogen-containing compounds via reaction (III) cannot compete with their sink via reaction (II).

REFERENCES

1. *Energii razryva khimicheskoi svyazi. Potentsial ionizatsii i srodstvo k elektronu* (Bond Dissociation Energies, Ionization Potential, and Electron Affinity) Kondrat'ev, V.N., Ed., Moscow: Nauka, 1974, p. 268.
2. Chameides, W.L. and Davis, D.D., *J. Geophys. Res.*, 1980, vol. 85, no. C12, p. 7383.
3. Danielsen, E.F., *J. Geophys. Res.*, 1993, vol. 98, p. 8665.
4. Chatfield, R.B. and Crutzen, P.J., *J. Geophys. Res.*, 1990, vol. 95, no. D18, p. 22319.
5. Maguin, F., Mellouku, A., Laverget, G., et al., *Int. J. Chem. Kinet.*, 1991, vol. 23, no. 3, p. 237.
6. Barnes, I., Bonsang, B., Brauers, T., et al., *Air Pollution Research Report*, 1991, vol. 35, p. 8.
7. Buben, N., Larin, I.K., and Trofimova, E.M., *Kinet. Katal.*, 1995, vol. 36, no. 6, p. 812.
8. Buben, S.N., Larin, I.K., Messineva, N.A., and Trofimova, E.M., *Khim. Fiz.*, 1989, vol. 8, no. 9, p. 1234.
9. Sturges, W.T. and Barrie, I., *Atmos. Environ.*, 1988, vol. 22, p. 1101.
10. Buben, S.N., Larin, I.K., Messineva, N.A., and Trofimova, E.M., *Khim. Fiz.*, 1990, vol. 9, no. 1, p. 116.
11. Atkinson, R., Baulch, D.L., Cox, R.A., Hampson, R.F., Kerr, K.A., and Troe, J., *J. Phys. Chem. Ref. Data*, 1992, vol. 21, p. 1125.
12. Buben, S.N., Larin, I.K., Spasskii, A.I., Trofimova, E.M., and Turkin, L.E., *Khim. Fiz.*, 2002, vol. 21, no. 4, p. 59.
13. Buben, S.N., Larin, I.K., Messineva, N.A., and Trofimova, E.M., *Khim. Fiz.*, 1996, vol. 15, no. 1, p. 116.
14. Larin, I.K., Messineva, N.A., Spasskii, A.I., Trofimova, E.M., and Turkin, L.E., *Kinet. Katal.*, 2000, vol. 41, no. 4, p. 485 [*Kinet. Catal.* (Engl. Transl.), vol. 41, no. 4, p. 437].